MNE 19 (2023) 100211

Contents lists available at ScienceDirect

Micro and Nano Engineering

journal homepage: www.sciencedirect.com/journal/micro-and-nano-engineering

Research paper

Robust sub-100 nm T-Gate fabrication process using multi-step development

Kaivan Karami [a,*], Aniket Dhongde [a], Huihua Cheng [a], Paul M. Reynolds [a], Bojja Aditya Reddy [b], Daniel Ritter [b], Chong Li [a], Edward Wasige [a], Stephen Thoms [a]

[a] University of Glasgow, Glasgow G12 8QQ, United Kingdom
[b] GenISys GmbH, Eschenstr. 66, 82024 Taufkirchen, Germany

ARTICLE INFO

Keywords:
Sub-100 nm T-Gate
Tri-layer resist stack
Multi-development

ABSTRACT

We demonstrate the fabrication of sub-100 nm T-Gate structures using a single electron beam lithography exposure and a tri-layer resist stack - PMMA/LOR/CSAR. Recent developments in modelling resist development were used to design the process, in which each resist is developed separately to optimise the resulting structure. By using a modelling approach and proximity correcting for the full resist stack, we were able to independently vary gate length (50-100 nm) and head size (250-500 nm) at the design stage and fabricate these T-Gates with high yield.

1. Introduction

III-V compound semiconductor-based high electron mobility transistors (HEMTs) have become workhorses of many applications for their superior speed and noise performance. For example, GaN HEMTs are widely used in both microwave devices and power electronics [1] and GaAs and InP HEMTs are extensively used in microwave and millimetre-wave front ends [2]. One of the most important steps in the fabrication process of high frequency HEMTs is forming the gate. Unity gain cut-off frequency (f_t) is related to the effective saturation velocity v_{sat} and the gate length (L_G) from Eq. (1) [3]. While v_{sat} is a material property, gate length can be used to scale the cut-off frequency. The shorter the gate length the higher the frequency, however short gate lengths increase access resistance as shown in Eq. (2). Thus, a T-shaped gate with bigger head and smaller foot has become the mainstream technology for high frequency HEMTs.

$$f_T = \frac{v_{sat}}{2\pi L_G} \tag{1}$$

$$R_G = \rho \cdot \frac{W_G}{L_G h} \tag{2}$$

Where R_G is the gate resistance, ρ is the resistivity of the metal, W_G is the gate width, L_G is the gate length, and h is the height of the gate.

These T-shaped gates (T-Gates) are among the most important structures in ultra-fast HEMTs [2,4] and are generally fabricated using electron beam lithography (EBL), due to its maskless exposure, high resolution, stability, flexibility, and precision registration [5]. Both electron forward scattering and mechanical stability [6] and gate pad bloating [7], limit shortening the foot. The use of a supporting dielectric between the head and channel is one potential solution, but has drawbacks of increased process complexity, increased gate-channel capacitance, and electrical damage to the channel caused by the etching of the dielectric [8,9]. Alternatively, some researchers opting for a single-step process tends to result in an increase in the fabricated gate foot size compared to the intended design [10,11].

There are two main steps in the T-Gate fabrication process. The first is to use lithography to create T-shape profiles in resists, and the second is to use metallization and lift-off to transfer the resist profile into metallic gates. The fundamental idea behind producing T-shaped profiles in a bilayer of resists using EBL is based on the variation in electron-beam sensitivity between the two layers of resists, with the upper resist layer being more sensitive than the lower. After development, the upper layer with higher sensitivity produces the broader head of the T-shaped gate, while the less sensitive lower layer forms the narrower foot. This profile is the inverse of the undercut process required for lift-off, so additional measures are generally taken to ensure a suitable undercut in the upper resist layer.

This study presents a CSAR/LOR/PMMA (CSAR is Allresist GmbH AR-P 6200 series resist; LOR is Kayaku Lift-off Resist, PMMA is poly

* Corresponding author.
E-mail address: kaivan.karami@glasgow.ac.uk (K. Karami).

https://doi.org/10.1016/j.mne.2023.100211
Received 8 January 2023; Received in revised form 12 May 2023; Accepted 22 May 2023
Available online 29 May 2023

(methyl Methacrylate)) resist stack for single-step EBL T-Gate fabrication, giving rise to a robust T-Gate manufacturing process. Tuning of the relative resist sensitivities is made possible by using independent development stages for the CSAR and PMMA layers. The LOR parting layer provides a controllable undercut in addition to separating the head and foot developments. 3D proximity correction was carried out using BEAMER [12].

2. Method and fabrication

The substrates used consisted of a 3 μm GaN structure on silicon. Multilayer resist stacks consisting of 150 nm PMMA (950 k), 300 nm LOR-3A and 250 nm CSAR were prepared, as shown in Fig. 1. The hotplate soft-bake settings were 5 min at 180 °C for the PMMA, and 2 min at 150 °C following each of the other two layers. After electron beam exposure using a Raith 100 kV EBPG 5200 electron beam lithography tool, development was carried out in three separate steps for the three resist layers. This enabled each layer to be developed independently, giving fine control over their relative sensitivities. CSAR was developed by dipping in a bath of amyl acetate at 23 °C for 30 s, followed by 30 s rinse steps in baths of isopropyl alcohol (IPA) and a blow dry. LOR-3A is not electron-sensitive, but is removed in a controlled way using TMAH, in this case using CD-26 for 25 s, followed by two 30 s rinse steps in baths of RO water. Finally, the PMMA was developed using IPA: MIBK 3:1 at 23 °C for 30 s, followed by an IPA rinse and a blow dry.

Initially the CSAR and PMMA resists were characterised individually by writing dose wedges consisting of 200 × 500 μm rectangles arrayed out at on a 400 μm period. A single profilometer scan was used to measure the remaining resist thickness after development. The contrast data from these scans was entered into the BEAMER software [12] together with the electron point spread function for the resist stack and material system. This enabled it to carry out 3-D Proximity Effect correction and calculate the correct foot and head doses to arrive at the desired structure. This becomes particularly useful for high-density areas, such as the gate feeds or where the gate pitch is small. Besides the correction these inputs were used to model the resist cross-section after development, using the GenIsys LAB modelling software [13].

The design of the T-structures was a central line at high dose for the foot. The head consisted of a wing on either side, written simultaneously with the same beam, but at a lower dose. The digital design had no gap between the foot and the wings. Each individual T-structure comprised a 4000 μm wide section for cleaving, and several narrower sections for direct SEM inspection. The base pattern consisted of a series of T-Gate structures with foot lengths between 50 and 100 nm, and head lengths from 250 to 500 nm. The complete pattern was a linear repeat of the base pattern written at different doses in such a way that all the gates could be sectioned with a single cleave.

The patterns were cleaved through the gates after development, and one half was coated with 2 nm Pt for cross-section Scanning Electron Microscope (SEM) inspection. Ni/Au (20/300 nm) metal layers were deposited by e-beam evaporation on the other half of the cleaved sample, to form a Schottky contact, followed by lift-off in warm acetone. These completed gates were inspected at an angle of 70° by SEM.

3. Results and discussion

Fig. 1 shows the contrast curves obtained for CSAR and PMMA resists. The clearing doses of the two resists were found to be 180 and 510 μC/cm^2 respectively, which gives a sensitivity ratio of 510/180–3 between the two resists. Because the two resists are developed independently, this ratio could easily be varied. For instance, the PMMA development step could be carried out at low temperatures, which is known to decrease the sensitivity [14] by up to a factor of 10. Alternatively, by developing in 1:1 IPA: water for 30s, the resolution remains similar but the sensitivity is increased by a factor of 1.4 [15]. Thus, without even varying the CSAR development, the sensitivity ratio can be varied between 2 and 30.

This is important because there is an optimum region of sensitivity ratio. If it is too low, then it becomes difficult to separate the head and foot processing and the process window for a well-formed T-structure with a controlled gate length becomes small. Taken to its ultimate limit, it is impossible to form a T-structure with a sensitivity ratio of 1. Conversely, if the ratio is too large, then there is a danger of the head layer 'bloating' when larger structures such as the gate feeds are written [7]. This is caused by the backscattered electrons from the large dose required to write the gate feed at the foot dose. We found that a sensitivity ratio of 3 gave excellent foot-length control while avoiding any issues with bloating.

Fig. 2a shows a cross section of LAB simulated development of a T-Gate with 50 nm gate foot. The development times for each layer were set to be the same as the experiment data. After the experimental sample got developed, it is sputtered with 2 nm Pt (platinum) to be able to see the cross section in SEM. Fig. 2b shows the SEM image of the cross section of the developed resist profile for 50 nm T-Gate. The simulated

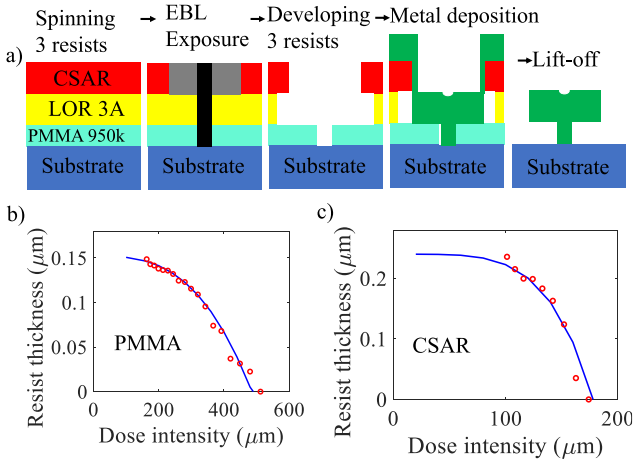

Fig. 1. (a) Resist stack and fabrication outline; smoothed contrast curves for (b) PMMA and (c) CSAR.

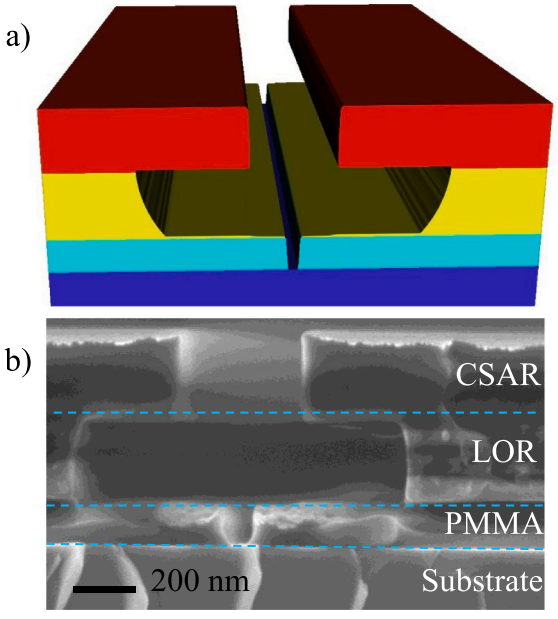

Fig. 2. Cross section of developed images of 50 nm gate foot with 294 μC/cm^2 dose exposure and using 30 s Amyl Acetate, 25 s in MF319 and 30 s in MIBK. a) LAB simulated cross section, b) SEM image of developed resist profile.

resist profile matches closely to the experiment developed resist profile demonstrating the benefit of using modelling software. Reducing the gate foot to sub 50 nm is possible using this resist stack from the resist image point of view but the mechanical stability of sub-50 nm metallised gates is reduced, and they are prone to topple, for instance during the blow-dry procedure when surface tension forces are significant. Supporting wider gate heads becomes increasingly challenging with reduced gate foot lengths and to minimise the risk of toppled gates we can design the T-Gate with foot to head size ratio of 1:3.

The developed sample was metallised with Ni/Au 20/300 nm using electron-beam evaporation technique to form the T-Gate metal stacks, followed by lift-off. The lift-off was easy and resulting in >98% yield of T-Gates over a wide range of design sizes and base doses. The results were shown well-defined T-Gate profiles using our new resist stack. Using this process, variations of foot and head sizes does not require separate process using this resist stack. Table 1 summarises the fabrication results for a number of T-Gates with designed 50 nm and 100 nm gate foot sizes and designed gate heads varying from 250 to 500 nm. It gives results for two base doses of 294 μC/cm^2 and 414 μC/cm^2. The data preparation assumed a base dose of 294 μC/cm^2, and this gave results closer to the designed structure compared to the increased dose (414 μC/cm^2). The 41% increase in dose gave rise to a 22% increase in gate length for the 50 nm gates, which demonstrates a robust process latitude. From the gate head measurements for both dose exposures, we can see that the measured gate heads are larger by >50 nm compared to designed gate heads. This is partly because the measured value in the table is from the bottom part of the gate head where there are small edges created after metallization on both sides (wings) as could be seen in Fig. 2. These edges don't affect the T-Gate performances when they are used in the devices. This resist stack could be used for high frequency devices where repeatability and mechanically stable of sub-100 nm T-Gate are required. Scaling further the gate foot to sub-50 nm dimensions is perhaps the most important future application scenario and the limitations here are discussed in the paper.

Fig. 3 shows SEM images of fabricated T-Gate fabricated using a base dose of 294 μC/cm^2. The designed foot length varies by column, and the head size by row. In Table 1, the measured foot heights are also shown for corresponding dose and T-Gate. It should also be noted that measurement of the foot length and height is difficult because the foot is under the head and can only be seen at the end of the gate structure. This leads to an error in the length measurement of around ±4 nm, as estimated from the data.

These measurements show a loss of 30–50 nm of PMMA resist thickness based on the fact that 150 nm PMMA is deposited and so the head height above the substrate is expected to be 150 nm. Some resist loss is expected because of the exposure of gate head (CSAR layer) which interacts with the PMMA foot layer. The development rate of PMMA varies as dose^g, where g, the contrast, is 2.7. With a sensitivity ratio of 3, the actual dose experienced by the PMMA adjacent to the foot is around 40% of the clearing dose, leading to an expected thinning of 12 nm. Additional AFM measurements of the resist profile show a resist loss of around 10–20 nm, which is closer to expectation. The difference may be caused by measurement uncertainties, such as the location of a baseline for the height measurement.

4. Conclusions

This paper describes a novel nanofabrication technique for T shape gates, which are a key component in III-V HEMTs. The fabrication process employs a CSAR/LOR/PMMA resist stack and yields robust 50 nm T-Gate structures. This single step electron beam writing process with multiple development steps minimises writing time and complexity. It also allows the sensitivity ratio to be adjusted to the optimum range, thus avoiding the twin evils of poor gate length control, and bloat around larger features such as gate pads. 3D proximity correction and modelling were employed and enabled the doses to be established prior to final T-Gate fabrication.

Table 1
Summary of measurements of T-Gate dimensions for two different base doses. In all cases the target foot height was 150 nm.

Foot length (nm)			Gate head (nm)			Foot height (nm)	
Design	294 μC/cm^2	414 μC/cm^2	**Design**	294 μC/cm^2	414 μC/cm^2	294 μC/cm^2	414 μC/cm^2
50	52	68	250	317	304	110	117
50	55	59	350	402	414	110	110
50	47	61	450	506	522	112	100
100	102	119	300	341	363	114	105
100	89	106	400	456	463	104	115
100	104	110	500	543	575	113	111

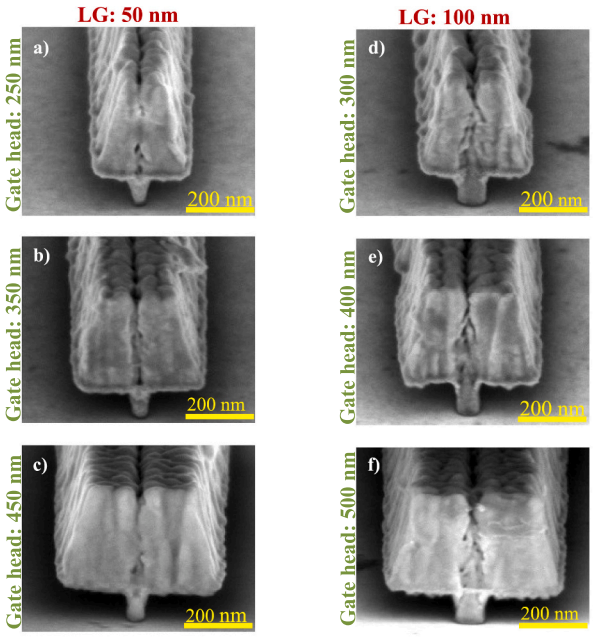

Fig. 3. SEM images at 75-degree angle of fabricated T-Gates after metallization and lift-off. There are two different gate foots 50 nm and 100 nm as indicated on the top of the images and different gate heads as indicated next to each image.

Declaration of Competing Interest

The authors declare that they have no known competing financial interests or personal relationships that could have appeared to influence the work reported in this paper.

Data availability

No data was used for the research described in the article.

Acknowledgement

The authors thank the staff of the James Watt Nanofabrication Centre (JWNC) at the University of Glasgow. This work was supported in part by EPSRC grant no. EP/R024413/1.

References

[1] X. Pang, et al., Bridging the terahertz gap: photonics-assisted free-space communications from the submillimeter-wave to the mid-infrared, J. Lightwave Technol. 40 (10) (2022) 3149–3162.

[2] I.G. Thayne, et al., Comparison of 80-200 nm gate length Al/sub 0.25/GaAs/GaAs/(GaAs: AlAs), Al/sub 0.3/GaAs/In/sub 0.15/GaAs/GaAs, and In/sub 0.52/AlAs/In/sub 0.65/GaAs/InP HEMTs, IEEE Trans. Elect. Dev. 42 (12) (1995) 2047–2055.
[3] F. Marino, N. Faralli, D. Ferry, S. Goodnick, M. Saraniti, Figures of merit in high-frequency and high-power GaN HEMTs, J. Phys. Conf. Ser. 193 (1) (2009) 012040. IOP Publishing.
[4] H.-B. Jo, et al., $L_g = 87$ nm InAlAs/InGaAs high-Electron-mobility transistors with a g_{m_max} of 3 S/mm and f_T of 559 GHz, IEEE Elect. Device Lett. 39 (11) (2018) 1640–1643.
[5] Y. Chen, Nanofabrication by electron beam lithography and its applications: a review, Microelectron. Eng. 135 (2015) 57–72.
[6] B. Cord, J. Yang, H. Duan, D.C. Joy, J. Klingfus, K.K. Berggren, Limiting factors in sub-10 nm scanning-electron-beam lithography, J. Vacuum Sci. Technol. B: Microelectron. Nanometer Struct. Proc. Measure. Phenomena 27 (6) (2009) 2616–2621.
[7] Y. Chen, D. Macintyre, S. Thoms, Effect of resist sensitivity ratio on T-gate fabrication, J. Vacuum Sci. Technol. B: Microelectron. Nanometer Struct. Proc. Measure. Phenomena 19 (6) (2001) 2494–2498.
[8] S. Bentley, X. Li, D. Moran, I. Thayne, Fabrication of 22 nm T-gates for HEMT applications, Microelectron. Eng. 85 (5–6) (2008) 1375–1378.
[9] M. Zhu, Y. Xie, J. Shao, Y. Chen, Nanofabrications of T shape gates for high electron mobility transistors in microwaves and THz waves, a review, Micro Nano Eng. 13 (2021), 100091.
[10] Y. Zhong, et al., Comparison of single-step and two-step EBL T-gates fabrication techniques for InP-based HEMT, Chin. J. Electron. 25 (2) (2016) 199–202.
[11] Y. Zhong, et al., T-gate fabrication of InP-based HEMTs using PMGI/ZEP520A/PMGI/ ZEP520A stacked resist, Chin. J. Electron. 25 (3) (2016) 448–452.
[12] N. Unal, D. Mahalu, O. Raslin, D. Ritter, C. Sambale, U. Hofmann, Third dimension of proximity effect correction (PEC), Microelectron. Eng. 87 (5–8) (2010) 940–942.
[13] GenISys. "Lithography Simulation & OPC."GenISys.https://www.genisys-gmbh.com/lab.html (accessed 01/05/2023, 2023).
[14] B. Cord, J. Lutkenhaus, K.K. Berggren, Optimal temperature for development of poly (methylmethacrylate), J. Vacuum Sci. Technol. B: Microelectron. Nanometer Struct. Proc. Measure. Phenomena 25 (6) (2007) 2013–2016.
[15] S. Yasin, D. Hasko, H. Ahmed, Comparison of MIBK/IPA and water/IPA as PMMA developers for electron beam nanolithography, Microelectron. Eng. 61 (2002) 745–753.